International Forum on Aeroelasticity and Structural Dynamics
IFASD 2024
17-21 June 2024, The Hague, The Netherlands

WIND TUNNEL TESTS FOR GUST LOAD INVESTIGATION IN TRANSONIC FLOWS – PART 2: EXPERIMENTAL RESULTS AND CONTROL DEMONSTRATION

Vincent Bouillaut[1], Alex Dos Reis de Souza[2], Pierre Vuillemin[2], Charles Poussot-Vassal[2], and Arnaud Lepage[1]

[1]DAAA, ONERA, Institut Polytechnique de Paris, 92320 Châtillon, France,
[2]DTIS, ONERA, Université de Toulouse, 31000, Toulouse, France.

Keywords: Wind tunnel tests, Gust load alleviation, Control

Abstract: Aerodynamic loads are a recurrent topic in aeronautical research. Indeed, during a flight, a wing can endure a wide variety of load sources impacting significantly the aerodynamical performances of the aircraft. Regarding those problematics, aeronautical studies aim to understand and find ways to decrease the effects of those disturbances. The present work focuses on one of those sources: the vertical gust, a particularly common phenomenon, responsible for important alterations of the airflow around the wing profile. To reproduce its effects, a gust generator has been installed in the contraction section of the S3Ch transonic wind tunnel at the ONERA Meudon center. The present study first introduces the gust generator used in this wind tunnel experiment. It is composed of two wings located upstream of the model. The two wings oscillate, hence creating vortices that will be carried by the flow stream to the model. Then, the effects of the gust are described, in both subsonic and transonic (up to Mach 0.82), on the aerodynamics and the aeroelastic response of a heavy instrumented (accelerometers, pressure sensors, strain gages) half wing fuselage model. In addition, an optical methodology gives access to deformation measurements of the model, thus giving a global picture of the phenomenon. Finally, a gust load alleviation methodology based on an active feedback loop is presented. A real-time device has been used and linked to a movable aileron of the model. A control algorithm based on several input sensors is implemented in the real-time device to decrease the effects of the gust load on the structural dynamics of the model. The results of this active control experiment will be discussed.

This work is part of the ”NACOR” project and has been funded within the frame of the Joint Technology Initiative JTI Clean Sky 2, AIRFRAME Integrated Technology Demonstrator platform ”AIRFRAME ITD”. The design and manufacturing of the innovative test rig is part of the associated project ”GUDGET”, with IBK-Innovation GmbH , Dream Innovation srl, Politecnico di Milano, Aviation Design and Cedrat Technologies SA as consortium partners.

1 INTRODUCTION

The main challenge in recent aeronautics is the reduction of fuel consumption. One way to achieve this goal is to reduce the induced drag by increasing their aspect ratio. Nevertheless, increasing aspect ratio comes with a counterpart as higher aspect ratio means more flexible wings, thus more responsive to aeroelastic effects, i.e. the impact of the surrounding airflow on the structural behavior. The path to cleaner aviation hence asks for in-depth study of the consequences of such shift.

The main phenomena investigated in aeroelastic studies are the triggering of instabilities which can be due to fluid-structure interactions (flutter, control surfaces inversion...), or the impact of external events on the wings such as gusts. Those are characterized by a sudden modification in the airflow, in the form of an ascending air flux impacting the wing from below. This phenomenon and its impact on the dynamic behavior of an airplane has been largely documented. It can lead to a significant reduction of the plane aerodynamic performances and/or threatening the structural integrity of the airplane. Due to such important risks to airplane safety, an important focus has been put in the design of methods to control, reduce or prevent the effect of gusts. To implement those methods, numerical simulations are useful tools ([1]) that require extensive experimental database to be developed, especially in transonic flows.

The present campaign is aimed at building such a database as well as testing control methods to reduce the effect of gusts on the dynamic behavior of a wing. To fulfill those goals, the first obvious objective is to be able to generate an upward flow velocity on the pressure surface of the wing. In the literature, several methods can be found to do so. In the present work, the gust generator consists in a pair of oscillating wings located upstream of the test section. Those motions result in the periodic creation of vortices, at the oscillation frequency. This manner of generating gusts can be related to [2] where two very close vane devices were used, or [3] at smaller speeds in 2004. At transonic speeds, [4] used oscillating vanes in 1990 that protrude from the tunnel walls. The characteristics of the gust generator, and the particularities of the half wing test model, will be presented in the second section, while the third section will show the results of the test campaign regarding the construction of the experimental database.

The last section will focus on the results regarding control methods to alleviate gust loads. Gust Load Alleviation (GLA) through active control techniques has driven a considerable attention in the literature since the 1970s. Indeed, one of the first implementation of an active GLA device dates back to 1977 [5]. It led to the incorporation of GLA systems in commercial airplanes such as the Tristar L-1011 [6] and the Airbus A320 [7]. Their popularity is due to their effect on reducing direct operating cost (6%) and fuel consumption (9%) [8]. Since then, numerous studies have been done on the matter ([9–18]), mostly in subsonic flows. One of the few GLA campaign in transonic flow was done at the ONERA Meudon center, within the framework of the european project *Clean Sky* (CS1) [19–21]. The present study relies on those previous results to further explore gust impact and GLA methods, as part of the NACOR project within the framework of *Clean Sky 2 AIRFRAME ITD* (CS2).

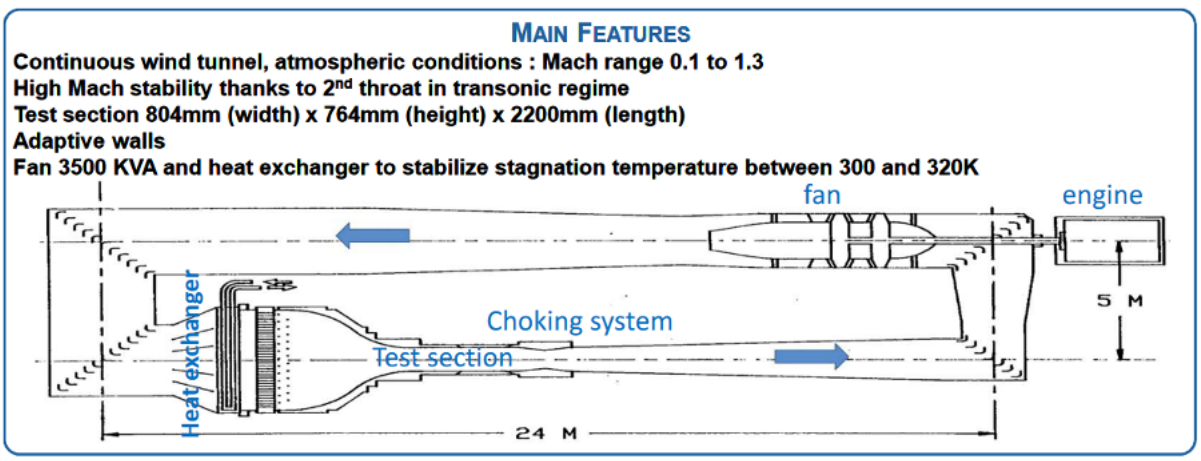

Figure 1: Schematics and main features of the ONERA S3Ch Wind Tunnel Facility.

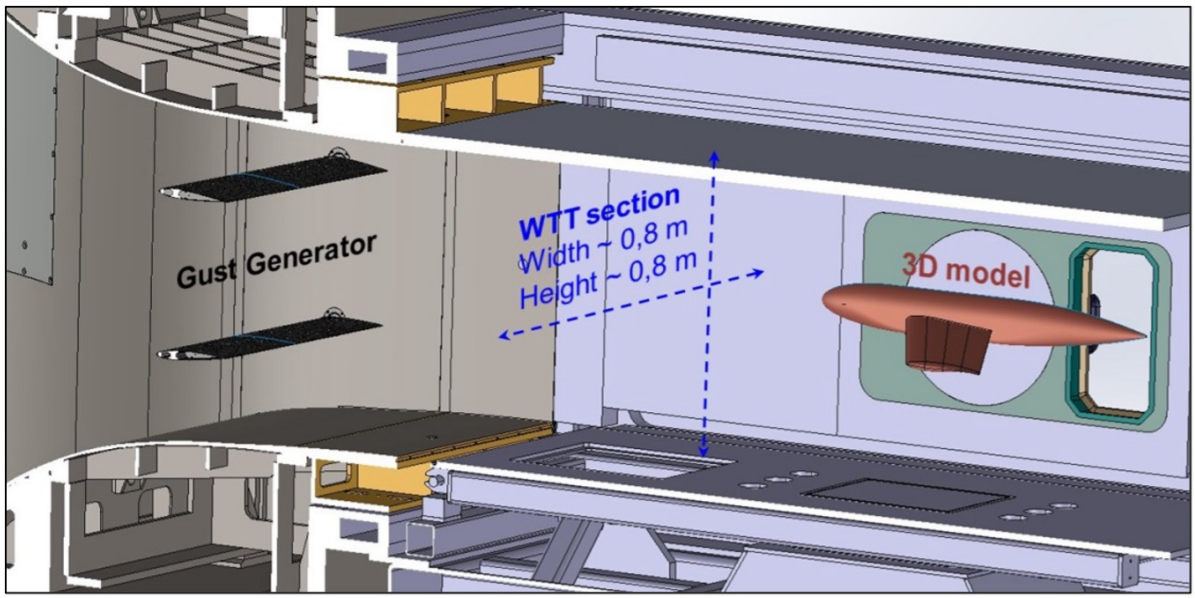

Figure 2: Overview of the test rig for the experimental gust load investigation.

2 EXPERIMENTAL APPARATUS

The campaign was carried out in the S3Ch transonic wind tunnel located in the ONERA Meudon center. The main features and a schematics of the facility are shown in Figure 1. Its main particularity is the adaptative walls that can be adapted to flow conditions to ensure a stable Mach number in the test section by reproducing far-field conditions. The flow velocity is adjusted by a downstream sonic throat, which warrants a $\pm 10^{-4}$ uncertainty on the Mach number. The test section is a 0.76x0.804x2.2m box where the Mach number domain extends from 0.3 to 1.2.

In the present campaign, several gust generation devices have been tested. They all share the same basic principle, it consists of two identical airfoils upstream of the test section as shown in Figure 2. One system had fluidic actuators located on both sides of the airfoils, pulsing air to disturb the circulation around it, hence creating vortices in its wake. Another was a variant of the one used in [21], a flap had been placed on the trailing edge of the airfoils, hence amplifying the effect of the device in creating vortices. The former failed to meet expectations while the latter, due to a malfunction during the experiments at transonic Mach numbers, had to be replaced by the one used in [21]. To assess the quality of the gust generators, the model is replaced by a clinometric probe, downstream of the gust generators, which measures the unsteady inclination of the flow. For a given set of parameters (amplitude and frequency of the fluidic or mechanical actuators), the performance of a device is defined by its ability to deviate the incoming flow, represented by the gust angle in the following.

The validation of both fluidic and mechanical gust generator devices, as well as their predicted performances at $M = 0.82$, can be seen in Figure 3, where the gust angle is plotted as a function of the command signal frequency. The fluidic devices were designed to compensate the lack of efficiency of mechanical devices at high frequencies. As shown in Figure 3, the measured performance of this device is indeed better suited for high frequencies. Nevertheless, when compared to the green curve (the predicted one), the measured performances were approximately 4 times inferiors to the expectations and only reaching the performances of the previous mechanical device (red curve). The blue curve is the prediction of the new mechanical device, designed especially for this campaign to be effective at low frequency.

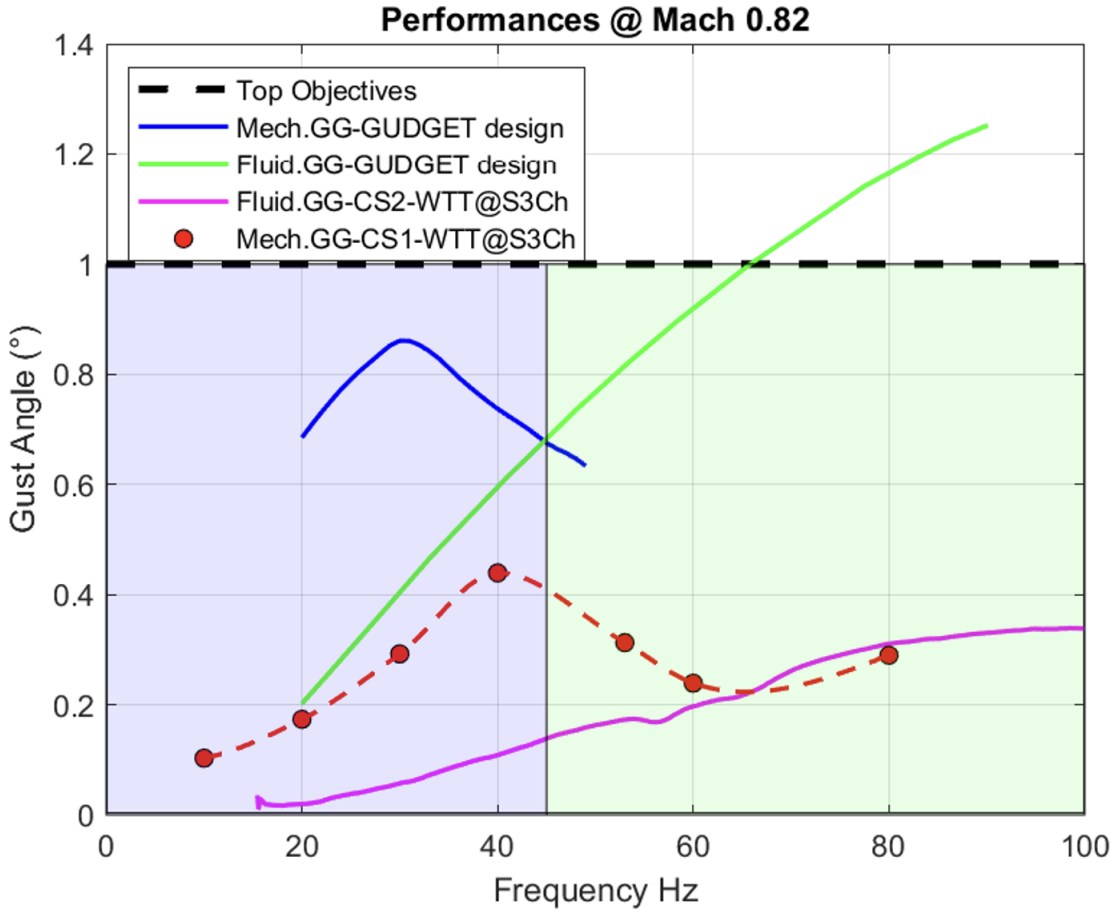

Figure 3: Summary of results in the form of gust angle as a function of frequency of the command signal: specifications, simulations and tests at Mach = 0.82. The dashed black line represents the objective of 1° gust angle. The blue and green curves represent the prediction (obtained via numerical simulations) of the newly designed mechanical gust generator (GG) and the fluidic GG, respectively. The red dashed curve and the pink one represent the measured gust angle for the GG used in CS1 and the fluidic GG, respectively.

The CS2 mechanical GG were then used but experimental contingencies led to replace the new mechanical design by one used in a previous GLA campaign, the CS1 mechanical GG. After this validation phase, the half wing model, presented in Figure 4, is placed in the test section in place of the clinometric probe. It is composed of a 3D swept wing and a fuselage, based on an ONERA geometry and manufactured from one main steel body. The wing and the fuselage are connected to a shaft allowing to tune the AoA or impose a dynamic pitch motion through an hydraulic actuator located at the end of the shaft line. To apply control methods, an aileron has been placed at the end of the wing to optimize its efficiency. During the validation and verification phase this aileron exhibited an angular deflection proportional to the static load, due to its inherent flexibility, hard to control while in flow. One of the particular feature of this model is the ability to add (or bypass) a specific pitch flexibility in the shaft line, hence adding a rigid body pitch mode in the dynamic.

This campaign had two objectives: building a comprehensive and relevant experimental database and investigate GLA with control approaches. To achieves those goals, the windless dynamic structural behavior has to be identified. A Ground Vibration Test (GVT) of the model has

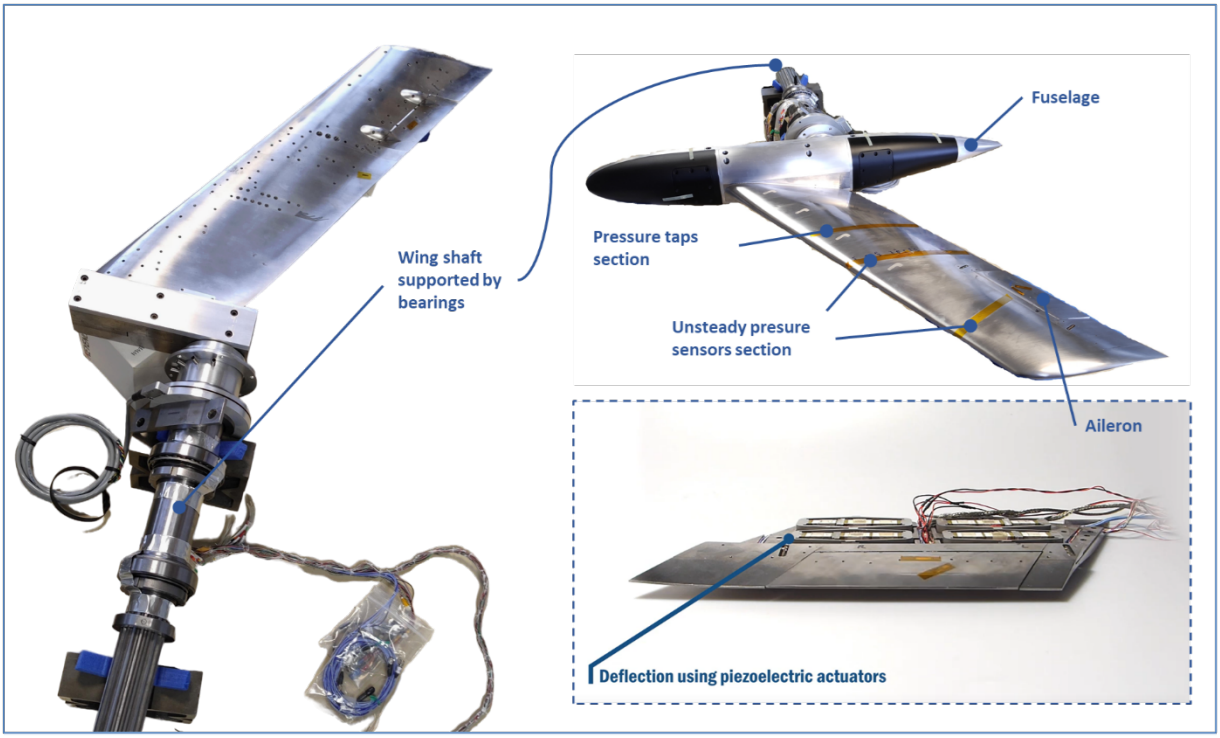

Figure 4: Overview of the half wing model equipped with the aileron and the fuselage.

thus been carried out in the experimental and structural dynamics laboratory in the ONERA Châtillon center prior to the wind tunnel experiments. The first structural modes are depicted in Figure 5 for both rigid and flexible configurations.

Once all the various components validated, the wind tunnel campaign can resume. The results are described in the next section.

3 RESULTS OF THE WING TUNNEL EXPERIMENTS

Model installation in the wind tunnel test section and test program. An overview of the experimental set-up is shown in Figure 6 presenting the wing installed in the test section and the "external components" of the setup (including supporting structures, electronic equipment and acquisition racks . . .). The WT test program was initially built in a parametric way to investigate several aerodynamic and aeroelastic configurations, incorporating variations of parameters:

- Mach Number with two main cases $M = 0.3$ and $M = 0.82$.
- Model angle of attack from $0°$ up to $4°$ with the ability to reach stabilized test point or to achieve slow AoA polar variations.
- Structural configurations driven by the state of the shaft coupling element (flexible vs rigid pitch boundary condition).

In the following, the results, figures and graphs, refer mainly to the transonic case, which is the most challenging one. As mentioned, the final database includes also similar results for low subsonic aerodynamic conditions.

Investigation of gust load. The next stage of the Wind Tunnel Test (WTT) campaign at the S3Ch facility was dedicated to the analysis of the gusts impact on the model's structural behaviour. Throughout this phase of the WTT, the Gust Generator operated actively to induce

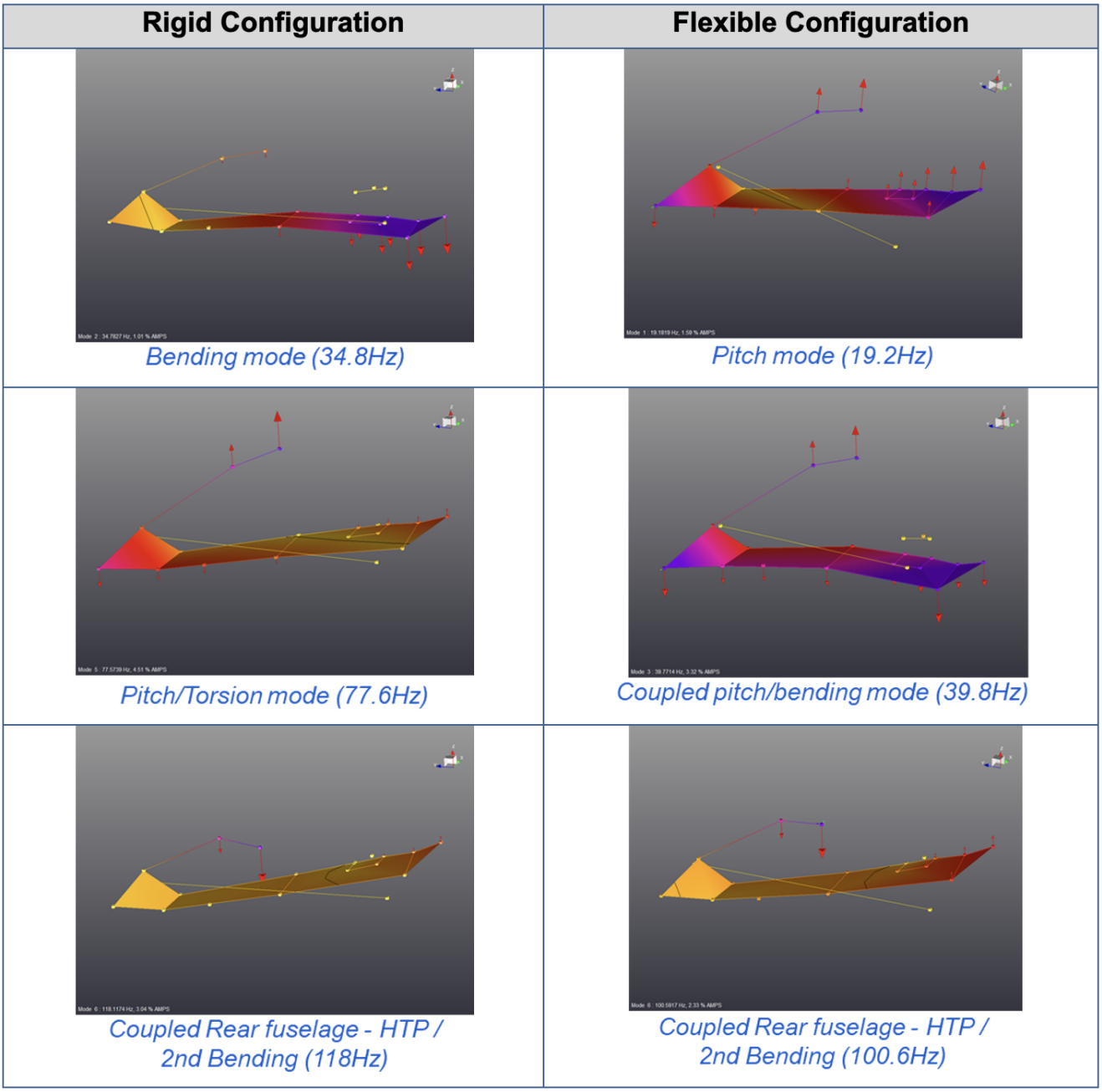

Figure 5: Modal organisation of the first three structural modes measured during the GVT.

gust perturbations that interacted with the wing.

Depending on the structural and aerodynamic conditions, a comprehensive database was acquired. With respect to gust disturbances, the test program was mainly conducted with harmonic gusts, whose frequency and amplitude parameters tailored the characteristics of the gust wave that propagated downstream.

Previous results have demonstrated the ability to generate a reproducible and significant gust field in the S3Ch facility. According to test campaign objectives, the model was then qualified in “rigid condition” to evaluate at first the aerodynamic phenomena induced by gust. The figures shown in Figure 7 show the pressure distributions for a sinusoidal gust generated at 20 Hz, impacting the model, for a transonic flow at Mach number 0.82 and for several angles of attack.

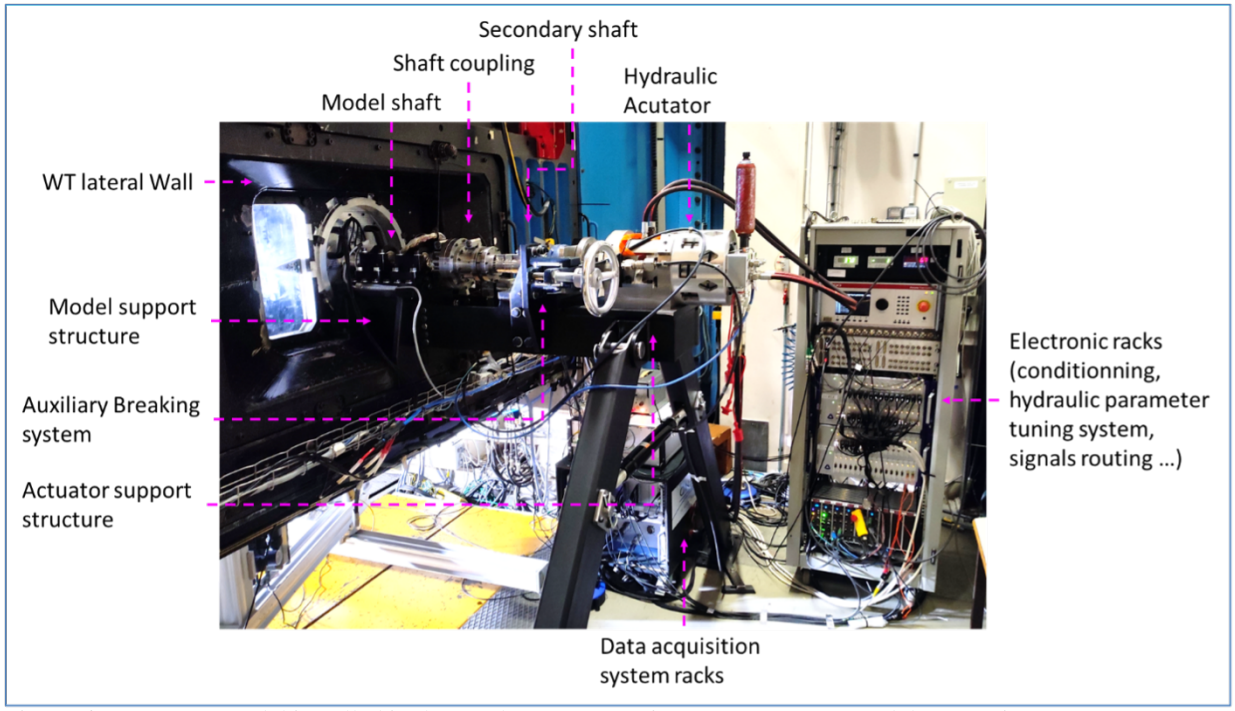

Figure 6: (Top) WT model installed in the S3Ch WT test section. (Bottom) WT model supporting structure assembly with all the main components and electronic devices for data acquisition.

Averaged values are superposed with instantaneous pressure measurements recorded at high sampling rate. The filled regions (grey and light red) cover the envelopes of the spatio-temporal evolutions of pressure coefficient fluctuations. As shown, the gust disturbance induced pressure

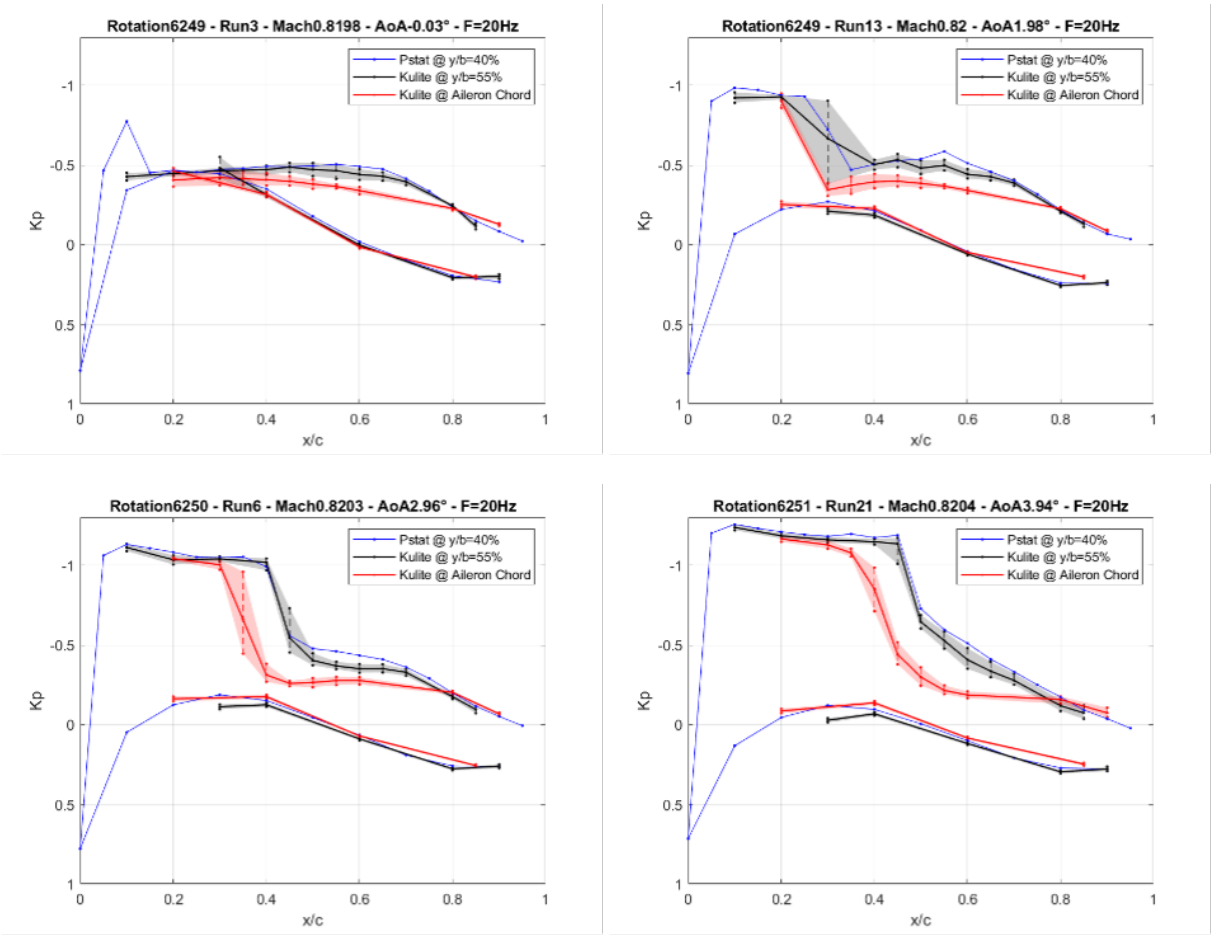

Figure 7: Pressure coefficient distributions at different angle of attack for Mach number M=0.82 and a harmonic gust @ 20Hz (solid curves represent averaged values; patch areas represent the envelope of instantaneous values).

fluctuations levels mainly located on the suction side of the model, in the shock location and downstream the shock foot. Depending on the angle of attack, the shock moved dynamically at the gust frequency with a chordwise motion between 5 and 10%. Similar results are depicted in Figure 8 in similar conditions but for a frequency generated at 80Hz. Discrepancies in terms of fluctuation levels are related to the difference of the gust amplitude depending of the driving frequency. A complementary visualization of the temporal data is shown in Figure 9 for M=0.82. The fluctuating parts of the instantaneous pressure coefficient distributions are represented for 20 periods of gust, generated at 80 Hz as a function of both sensor location and time. Depending on the angle of attack value, the effect of the gust on the pressure field is either entirely different or perceived differently depending on the sensor resolution:

- For AoA $= 0°$, the pressure fluctuations are located on the first half of the chord (between the leading edge and the mid chord),
- For AoA $= 2°$ and $3°$, the highest fluctuation levels are positioned on the shock and/or and at the shock foot. In the concerned AoA range, the shock location is very sensitive to the model's AoA or the flow angle (i.e. the gust angle). Some sensors are located very close to the shock location and oscillate between states related to the supersonic plateau

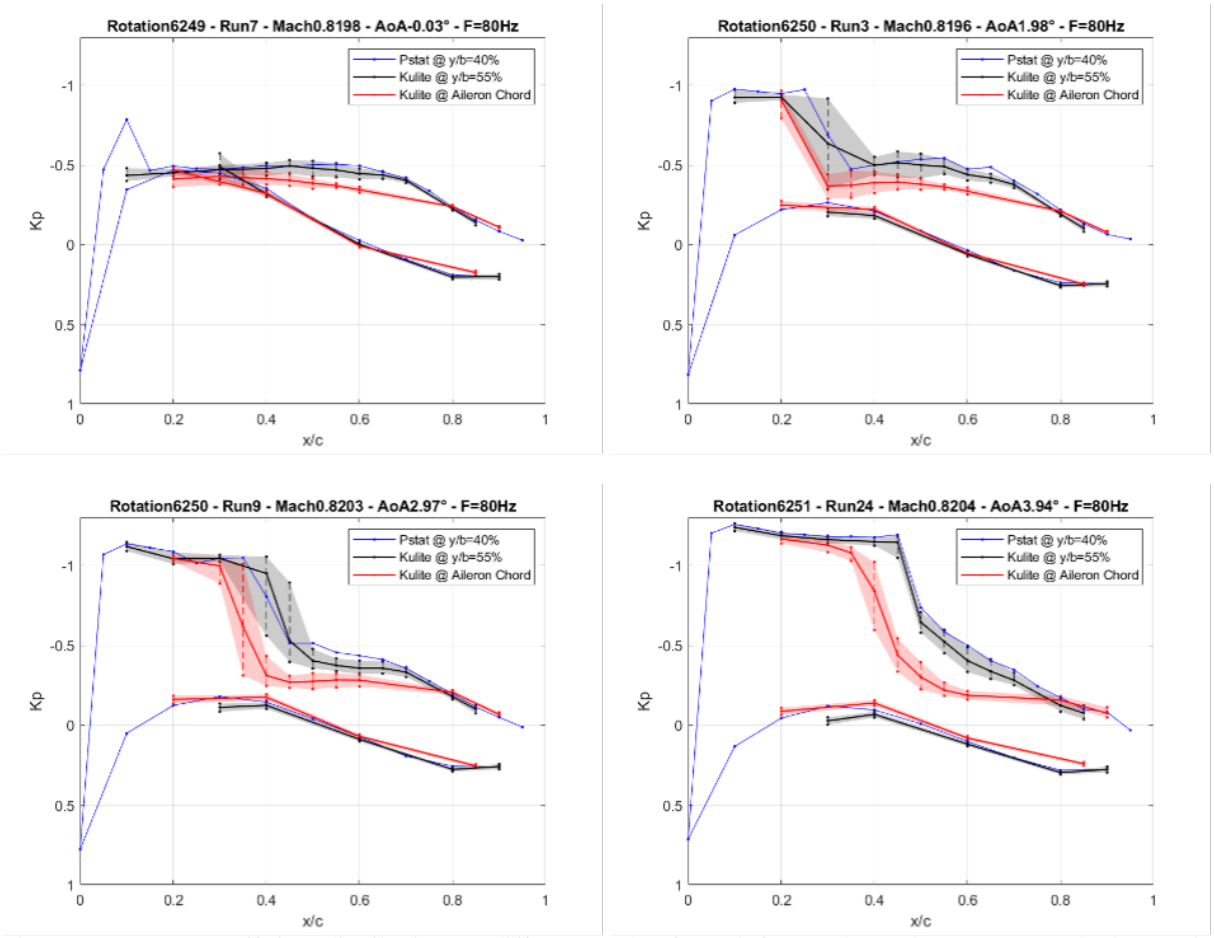

Figure 8: Pressure coefficient distributions at different angle of attack for Mach number M=0.82 and a harmonic gust @ 80Hz (solid curves represent averaged values; patch areas represent the envelope of instantaneous values).

or the shock foot, measuring large pressure fluctuations,

- For AoA $= 4°$, the shock on the upper surface is very intense, but its position appears to be quasi-insensitive to a small variation of the angle of attack around 4°. Similarly, the effects of the gust angle also seem to have little impact on the shock position. The maximum fluctuations are observed after the shock foot, over approximately 20-30% of the chord (possibly in a separated region).

Aeroelastic phenomena induced by gusts. For the investigation of aeroelastic phenomena induced by gust, the behaviour of the elastic wing motions was analysed under calibrated gust perturbations (main outcome of the CS1 WTT campaign). For different stable WT conditions (Mach, AoA) and both structural configurations, sine as well as sweep sine signals were used as input command. Some typical results for the embedded accelerometers and strain gauges responses are depicted in Figure 10 and Figure 11 for various test configurations (subsonic vs transonic flow, "rigid vs flexible" structural configuration). For sweep sine excitations, the gust command signal (frequency and amplitude) was modulated as functions of time to generate a gust amplitude over the wide frequency bandwidth as constant as possible. The first vibrational modes of the model can be seen in temporal signals of the wing's sensors for a gust perturbation. For both structural configurations, the highest response levels are observed in vicinity of the first wing bending mode located around 40 Hz. For the "flexible configuration", the presence of the pitch mode is clearly exhibited at 20 Hz and excited by the gust perturbation.

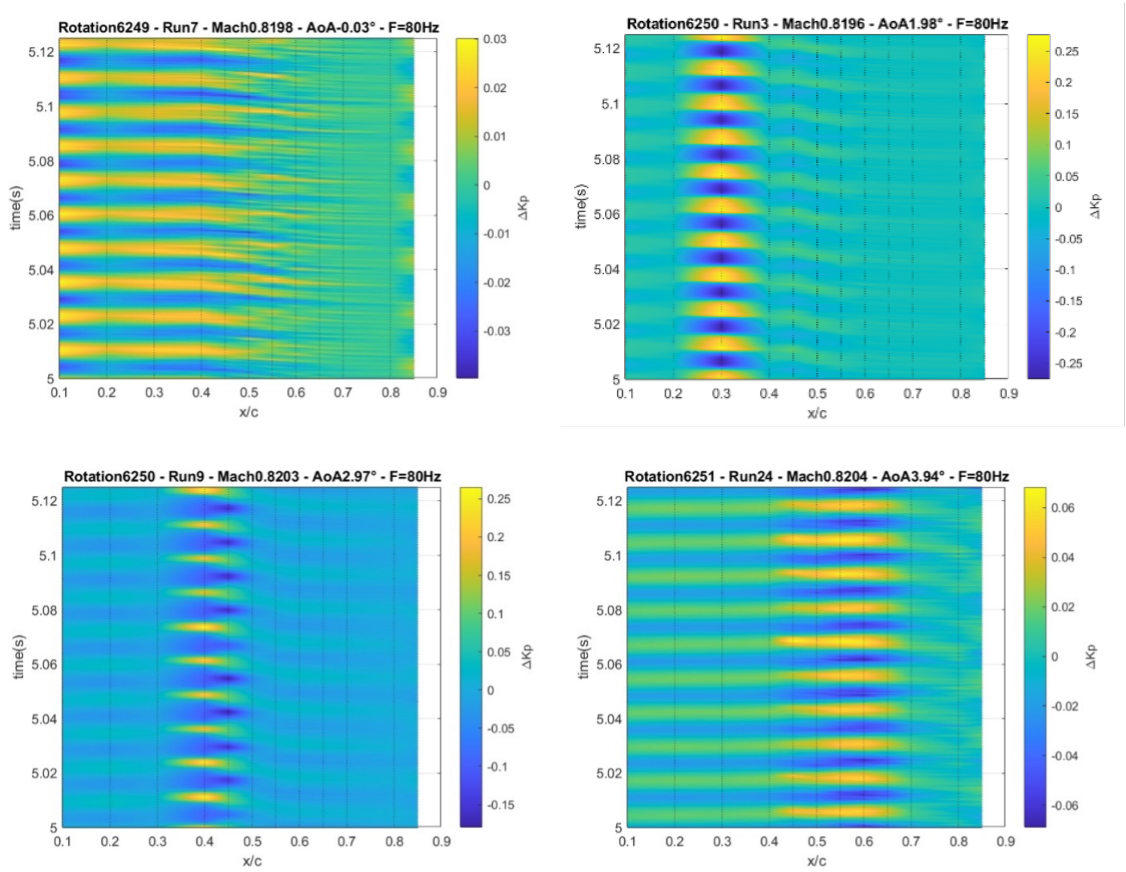

Figure 9: Spatio-temporal representation of pressure coefficient fluctuations $\Delta K_P(x/c, t)$ on the Kulite chord located at $y/b = 55\%$, for different angle of attack, Mach number $M = 0.82$ and a harmonic gust @ 80Hz.

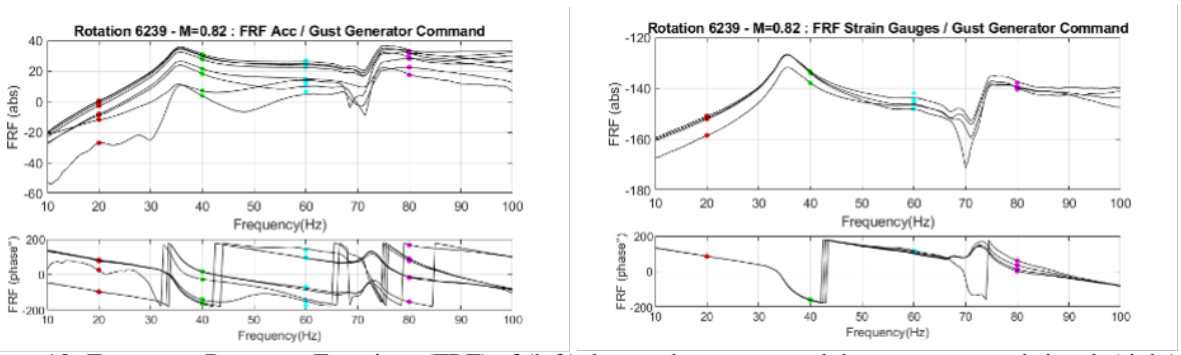

Figure 10: Frequency Response Functions (FRF) of (left) the accelerometers and the gust command signal, (right) the strain gauges and the gust command signal – Tests at M=0.82, AoA=0° - "Rigid structural configuration".

4 GUST LOAD ALLEVIATION

Gust Load Alleviation (GLA) was one of the objectives of the wind tunnel test campaign in the ONERA S3Ch facility and was achieved through a closed loop control (CLC) approach. The structure exhibiting a vibrational behaviour modified by the presence of gusts in the flow, the purpose of CLC algorithms was to target structural modes excited by gusts and damp the model's structural response amplitude in real time by imposing a complex oscillatory motion on the aileron. Those algorithms, based on advanced GLA functions that will be describe in a future paper, and the real-time platform were handled by several ONERA teams. In the following section, the real-time platform will be described as well as the implementation of the

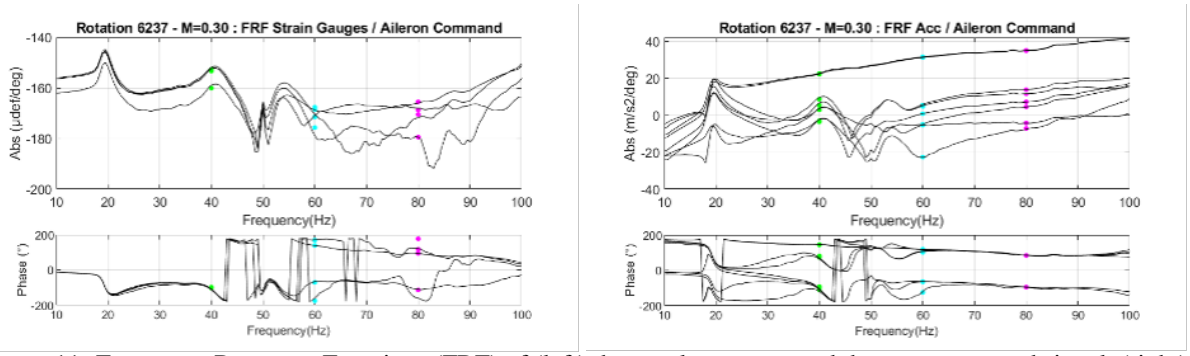

Figure 11: Frequency Response Functions (FRF) of (left) the accelerometers and the gust command signal, (right) the strain gauges and the gust command signal – Tests at M=0.3, AoA=0° - "Flexible structural configuration".

CLC algorithms.

Real time platform. The investigation of GLA demands to be able to receive data from the model, process them and send back a control signal to the aileron as fast as possible. It requires a special kind of device, a real-time controller, possessing multiple inputs/outputs and having a fast processing unit.

The platform used here is a dSPACE real-time controller composed of several cards (a computation card, an inputs card and an outputs card) divided in two modules able to communicate and sharing data with each other, as shown in Figure 12. The presence of two distinct modules allows to parallelize the computation and makes the real-time platform versatile. When using real-time platforms, the main concern is the amount of virtual memory used by the algorithms. Hence, having two different modules is a simple way to enhance the performance of the platform, by separating the tasks between the two. A computer is linked to the platform, monitoring the signal received and sent, and allowing to modify certain parameters during an experiment.

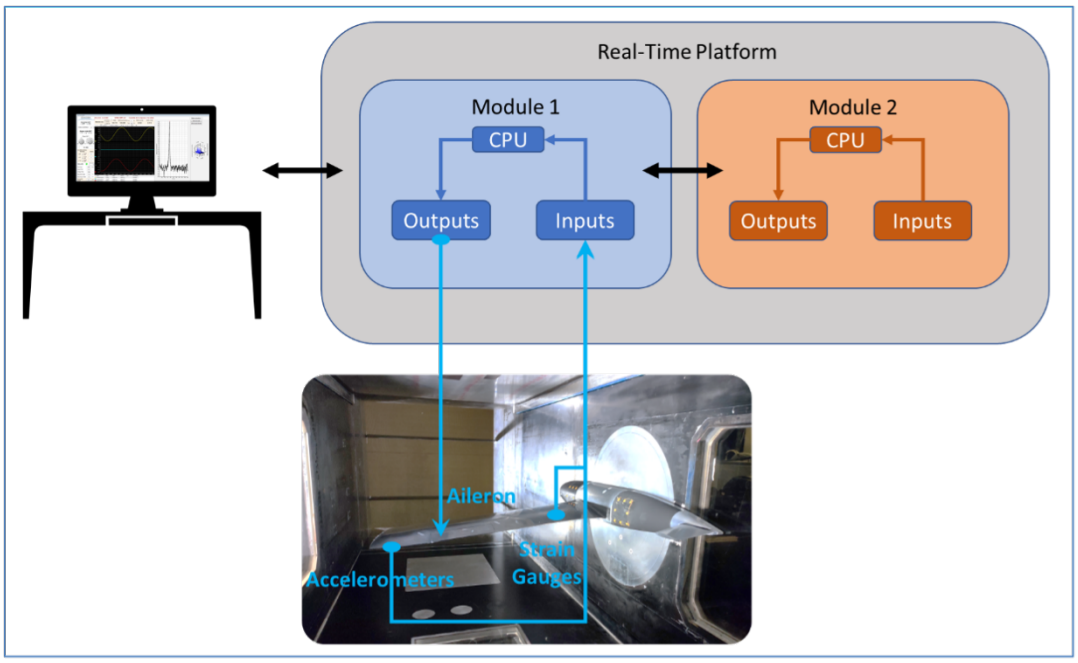

Figure 12: Diagram of the real time platform.

A large number of sensors are located at several locations inside the model and connected to the

real-time platform. Among them, certain accelerometers are chosen to perform GLA, certain strain gauges are chosen to monitor the control efficiency. Before arriving in the input card, the data is sent in an anti-aliasing filter to avoid sampling issue. Then, the data passes through the control algorithm implemented in the real-time platform to generate the control signal sent to the aileron.

Implementation of control algorithms and graphic user interface. The purpose of the real-time platform, in this campaign, was to be able to compute a control signal based on the measurements of the accelerometers, then sent it to the model's aileron. Different types of controllers were designed to be tested during the campaign. The implementation was done through a Simulink diagram composed of two sub-models, uploaded on the platform. The first one ensured the application of the control function. The control block took as input the measurements from a selection of embedded accelerometers. The output of the controller was directly sent to the input of the electronic device driving the aileron position. In order to assess different control algorithms, a simple parameter of the control interface allowed to switch between algorithms to be able to assess the efficiency of different control techniques during the experiment, without any new implementation or compilation, and without stopping the airflow. The mechanical parts ensuring the motion of the aileron being fragile (aileron kinematic and piezoelectric actuators), a security has been coded so that the control signal could not exceed a maximum value, this role was achieved by a saturation block.

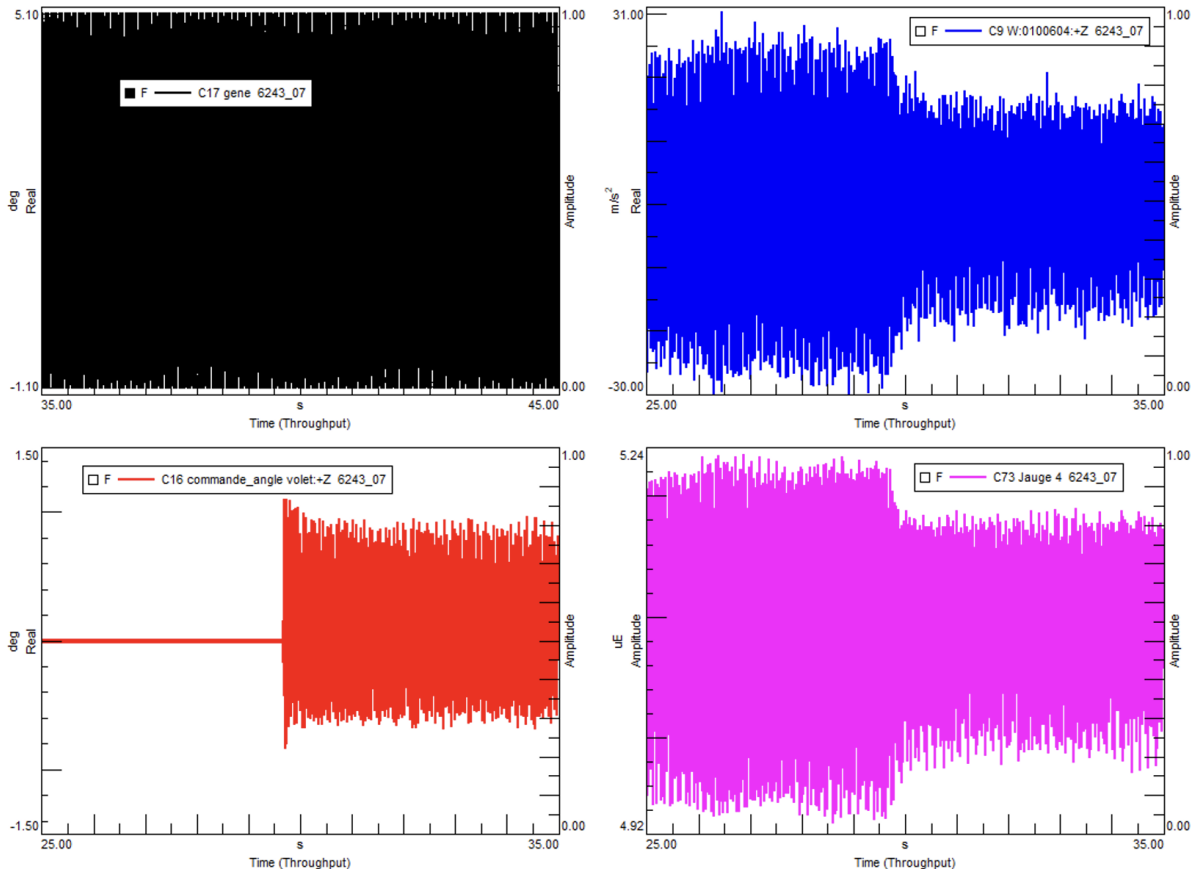

Figure 13: Illustration of GLA results for Mach $= 0.3$ and a gust disturbance @ 18.3Hz (Top left: Gust Generator Command – Bottom left: Aileron command – Top right: Accelerometer response – Bottom right Strain Gauge response).

Demonstration of GLA. In this part of the WTT program, the main objective was the demonstration, in real time, of the active control of the model aeroelastic response to a gust disturbance. At first, tests were carried out for the "flexible structural configuration". The control laws were designed to act on the pitch mode without impacting the higher modes (e.g. amplification of the first bending). An illustration of GLA in real time is presented in Figure 13 and Figure 14, for Mach numbers of $= 0.3$ and 0.82, respectively, and for a harmonic gust perturbation with a sinusoidal command locked on a frequency close to the pitch mode (i.e. model structural configuration = "flexible configuration"). The black curve refers to the GG command signal driving the harmonic motions of the GG and generating a gust field with an amplitude close to $\pm 0.6°$ for the subsonic case and $\pm 0.2°$ for the transonic case.

When the controller is switched on, the dynamic aileron deflection is activated by the controller output. A significant reduction of the model aeroelastic response is observed through embedded sensors (accelerometers and strain gages). Then the control efficiency was assessed for a wide

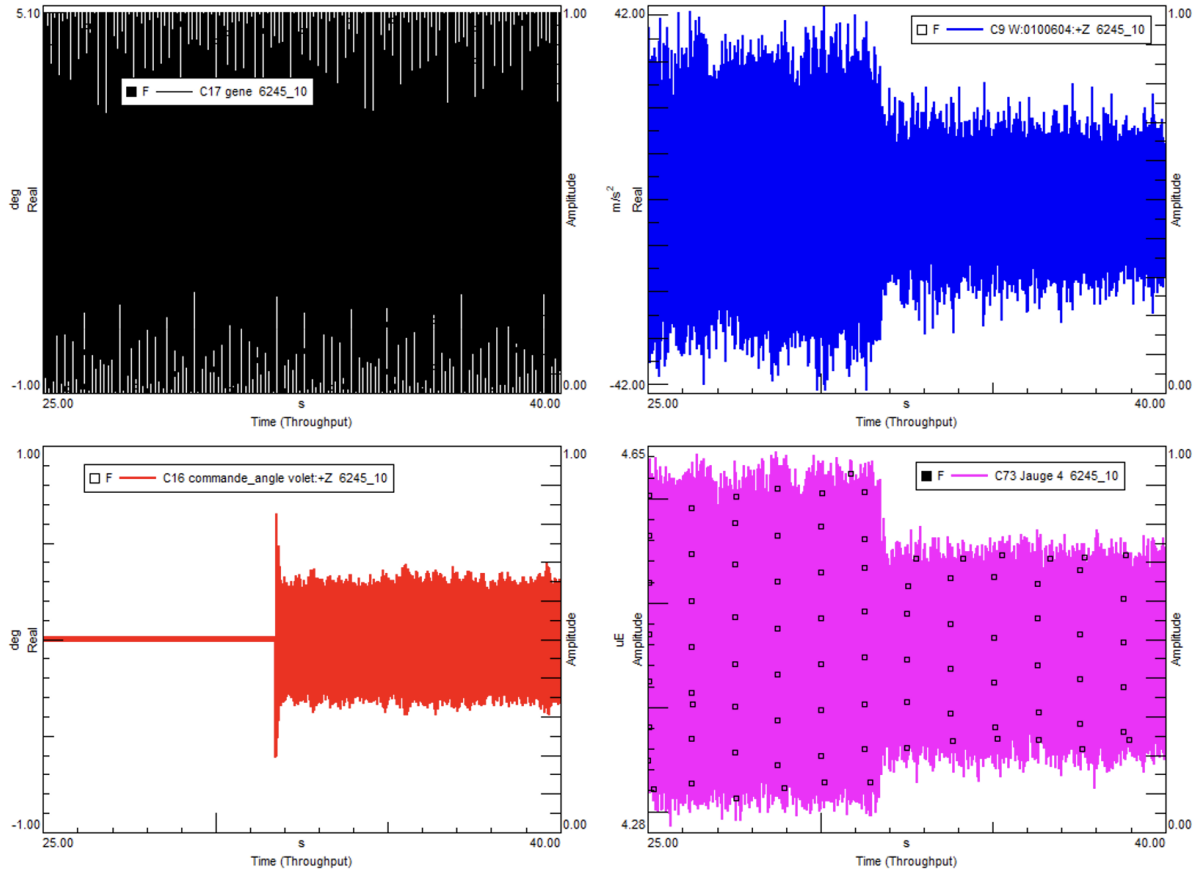

Figure 14: Illustration of GLA results for Mach $= 0.82$ and a gust disturbance @ 21.3Hz (Top left: Gust Generator Command – Bottom left: Aileron command – Top right: Accelerometer response – Bottom right Strain Gauge response).

band of gust excitations driven by a sweep sine command. Different types of control strategies were implemented in the real time platform. At first, the stability of the CLC system was verified over a wide frequency bandwidth. Typical results are depicted in Figure 15 for the subsonic case with three different kinds of controllers. The open-loop data (i.e. without control) are superimposed with the closed-loop data (with active control). As expected during the controller synthesis design, the control laws are efficient in vicinity of the first mode and no amplification appears at higher frequency.

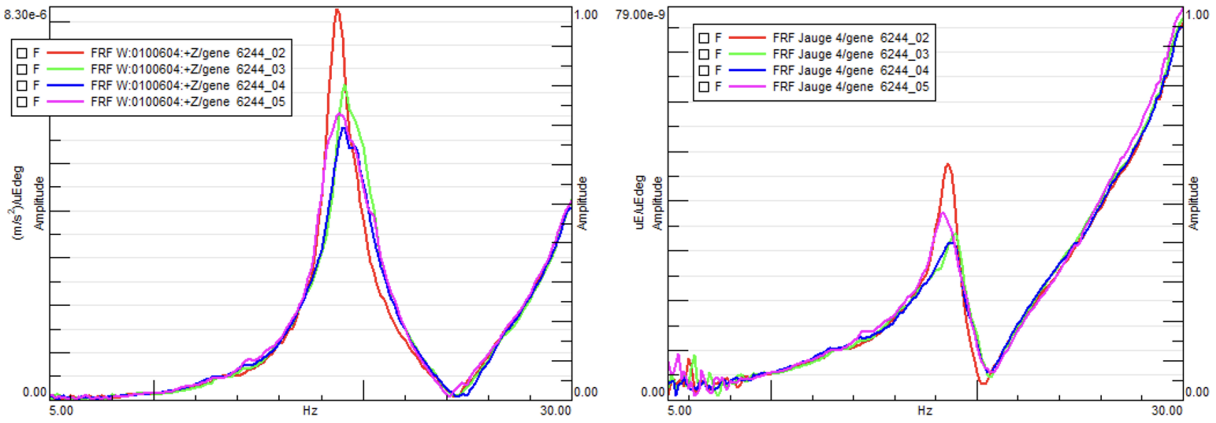

Figure 15: Illustration of GLA results for Mach = 0.3 and a gust driven by a sweep signal between 10 and 30 Hz (left: accelerometer response and right: strain gage response): No control (red), Controller 1 (green), Controller 2 (blue), Controller 3 (pink).

5 DISCUSSION

The analyses of the results and outcomes of the WTT campaign indicate that the tests provided a relevant and high-quality database. However, it is important to note that the testing encountered several challenges, and certain limitations reduced the complete fulfillment of the initial objectives. The low efficiency of the fluidic GG has been investigated during the campaign and several improvement axes have been identified. The re-utilization of the ”legacy” GG appeared to be a viable solution and allowed to perform the majority of the planned test program. Another challenge arose in the system used to set the rigidity of the pitch motion. As seen in Figure 6, this system is very complex and one of the bearings did loosen its grip on the shaft during the WTT. As the GLA tests were done at the end of the campaign, the team developing the control algorithm had to deal with a degraded modal organization. Nevertheless, as seen in Figures 15, control algorithms were successfully applied to the model and showed interesting results.

Complex designs lead to complex challenges. Some improvement need to be done in a future project regarding the GG devices and the WT model (occurrence of non-linear behavior) but this study represents a promising step in our understanding of transonic gusts and how to mitigate their effect.

6 REFERENCES

[1] Liauzun, C. (2010). Asme 2010 3rd joint us-european fluids engi- neering summer meeting collocated with 8th international con- ference on nanochannels, microchannels, and minichannels (american society of mechanical engineers).

[2] Ricci, C. and Scotti, A. (2008). 49th aiaa/asme/asce/ahs/asc structures, structural dynamics, and materials conference.

[3] Grissom, D. and Devenport, W. (2004). Developement and testing of a deter- ministic disturbance generator. 10th aiaa/ceas aeroacoustics conference.

[4] Mirick, P., Hamouda, M. N. H., and Yeager, W. (1990). Wind tunnel survey of an oscillating flow field for application to model helicopter rotortesting. Tech. Rep. TM 4224/AVSCOM TR 90-B-007, NASA.

[5] Disney, T. E. (1977). C-5a active load alleviation system. *Journal of Spacecraft and Rockets*, 14(2), 81–86.

[6] Johnston, J. (1979). Accelerated development and flight evaluation of active controls concepts for subsonic transport aircraft. volume 1: Load alleviation/extended span development and flight tests. Tech. rep.

[7] Payne, B. (1986). Designing a load alleviation system for a modern civil aircraft. *Proceedings of the 15th International Council of the Aeronautical Sciences, London, UK*, 7–12.

[8] Xu, J. and Kroo, I. (2011). Aircraft design with maneuver and gust load alleviation. In *29th AIAA Applied Aerodynamics Conference*. p. 3180.

[9] Demourant, F. and Ferreres, G. (2002). A frequency domain identification-control approach for a flexible aircraft. In *Proceedings of the International Conference on Control Applications*, vol. 1. IEEE, pp. 126–131.

[10] Moulin, B. and Karpel, M. (2007). Gust loads alleviation using special control surfaces. *Journal of Aircraft*, 44(1), 17–25.

[11] Torralba, J., Puyou, G., and Demourant, F. (2009). Self-scheduling multiobjective control law design for a flexible aircraft. In *AIAA Guidance, Navigation, and Control Conference*. p. 6303.

[12] Aouf, N., Boulet, B., and Botez, R. (2000). Robust gust load alleviation for a flexible aircraft. *Canadian Aeronautics and Space Journal*, 46(3), 131–139.

[13] Haghighat, S., Liu, H. H., and Martins, J. R. (2012). Model-predictive gust load alleviation controller for a highly flexible aircraft. *Journal of Guidance, Control, and Dynamics*, 35(6), 1751–1766.

[14] Giesseler, H.-G., Kopf, M., Faulwasser, T., et al. (2013). Gust load alleviation based on model predictive control. In *International Forum on Aeroelasticity and Structural Dynamics 2013 (IFASD)*.

[15] Demourant, F. and Ferreres, G. (2013). A linear parameter-varying multiobjective control law design based on youla parametrization for a flexible blended wing body aircraft. *Progress in flight dynamics, guidance, navigation, control, fault detection, and avionics*, 6, 729–748.

[16] Xu, J. and Kroo, I. (2014). Aircraft design with active load alleviation and natural laminar flow. *Journal of Aircraft*, 51(5), 1532–1545.

[17] Alam, M., Hromcik, M., and Hanis, T. (2015). Active gust load alleviation system for flexible aircraft: Mixed feedforward/feedback approach. *Aerospace Science and Technology*, 41, 122–133.

[18] Schirrer, A., Kozek, M., Demourant, F., et al. (2015). Feedback control designs. *Modeling and Control for a Blended Wing Body Aircraft: A Case Study*, 147–226.

[19] Brion, V., Lepage, A., Amosse, Y., et al. (2015). Generation of vertical gusts in a transonic wind tunnel. *Experiments in Fluids*, 56, 1–16.

[20] Poussot-Vassal, C., Demourant, F., Lepage, A., et al. (2016). Gust load alleviation: Identification, control, and wind tunnel testing of a 2-d aeroelastic airfoil. *IEEE Transactions on Control Systems Technology*, 25(5), 1736–1749.

[21] Poussot-Vassal, C., Vuillemin, P., Lepage, A., et al. (2022). Aircraft feedback gust load control design and experimental wing bench validation. In *AIAA Scitech 2022 Forum*. p. 1044.

ACKNOWLEDGEMENTS

The ONERA works have been funded within the frame of the Joint Technology Initiative JTI Clean Sky 2, AIRFRAME Integrated Technology Demonstrator platform ”AIRFRAME ITD” (NACOR project - contract N. CS2-AIR-GAM-2020-21-04) being part of the Horizon 2020 research and Innovation framework program of the European Commission.

The GUDGET project has received funding from the Clean Sky 2 Joint Undertaking under the European Union’s Horizon 2020 research and innovation programme under grant agreement No 831802.

The authors would like to thank J.C. Abart, F. Bouvier, Y. Amosse, C. Thémiot, Y. Remery, A. Konaté and L. Bouvier for their dedication during the WTT campaign.

COPYRIGHT STATEMENT